Proceedings of the 2014 IEEE
International Conference on Robotics and Biomimetics
December 5-10, 2014, Bali, Indonesia

Back Propagation Neural Network Dehazing

Jiaming Mai, Qingsong Zhu*, *Member*, *IEEE*, Di Wu, Yaoqin Xie, *Member*, *IEEE*, Lei Wang, *Member*, *IEEE*

***Abstract*— In this paper, we propose a novel learning-based approach for single image dehazing. The proposed approach is mostly inspired by the observation that the color of the objects fades gradually along with the increment of the scene depth. We regard the RGB values of the pixels within the image as the important feature, and use the back propagation neural network to mine the internal link between color and depth from the training samples, which consists of the hazy images and their corresponding ground truth depth map. With the trained neural network, we can easily restore the depth information as well as the scene radiance from the hazy image. Experimental results show that the proposed approach is able to produce a high-quality haze-free image with the single hazy image and achieve the real-time requirement.**

I. INTRODUCTION

In hazy weather, the clarity of the scenery objects is severely obscured by small suspended particles. Outdoor images taken in such bad weather condition are prone to be low-quality as shown in Figure 1(a), and this leads to the fact that most vision applications such as video-surveillance systems and traffic monitoring systems fail to work normally. To solve this problem, improving the technology of image dehazing is highly desired. Image dehazing is an effective approach to increase the visibility and recover the real radiance of the hazy image. Moreover, removing hazes from the hazy image will benefit many computer vision algorithms (e.g. image segmentation [1]). Therefore, it is significant to research on image dehazing.

There are quite a large number of efforts that have been spent on image dehazing. In the early years, researchers tend to use the technique of image processing such as histogram equalization and gamma transformation to remove hazes from the image [2-4]. As all of these traditional methods are physically invalid, the dehazing effect is limited to a great extent. For further improving the effect of dehazing, some methods that try to utilize more additional information are proposed. In [5-10], researchers remove hazes with multiple images taken in different weather conditions or different degrees of polarization. In [11, 12], significant efforts have been spent on the image dehazing methods which are based on the given depth information. Unfortunately, these methods are hard to be applied in applications. The main reason is that multiple images or additional information are not available in most cases.

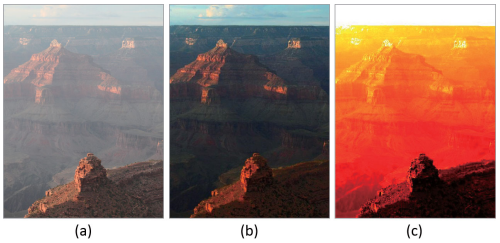

Fig. 1 Results of back propagation neural network dehazing. (a) The input hazy image. (b) Image after dehazing by our approach. (c) Our restored scene depth map.

In the past decade, there has been remarkable progress on model-based single image dehazing [13-20], which can benefit a lot of computer vision algorithms such as video segmentation[21] and image matting[22]. Assuming that the local contrast of the hazy images is much lower than that of the haze-free images in most cases, Tan [13] proposed to maximize the local contrast to remove hazes from a single hazy image. The results is compelling while they fall into oversaturated. Considering that the surface shading and the transmission are locally statistically uncorrelated, Fattal [14] proposed a novel single image dehazing algorithm which is physically sound. Although the algorithm can restore most details of the scenery objects, it fails to handle the dense-haze regions. Furthermore, it can only be used for color image dehazing. Based on the observation on a large amount of the haze-free images, He et al. [15, 16] presented the dark channel prior for single image haze removal. The dark channel prior is actually the statistics that in most of the patches where the sky is not present, there are several pixels whose values are close to zero in at least one color channel. The dehazing effect is pleasing, but it encounters difficulties to deal with sky region. Under the assumption that the scene depth in the local patch is continuous, Tarel et al. [17, 18] proposed a fast dehazing method based on the ”median of median filtering”. However, since such a strong assumption is often invalid, halos articles will appear near the depth discontinuities of the dehazed image. By creating a factorial Markov random filed (MRF) model of the image, Nishino et al. [19, 20] proposed a Bayesian method to estimate the depth information and the scene radiance from the input hazy image. The method is able to restore more details, but it is prone to produce oversaturated results in most cases.

Manuscript received September 12, 2014; accepted October 18, 2014. This work was supported in part by the National Natural Science Foundation of China under Grants 61303166), Shenzhen Key Lab for Computer Vision and Pattern Recognition under Grant CXB201104220032A), and by the National Basic Research 973 Program of China under Grant 2010CB732606)

J. Mai is with the Shenzhen Institutes of Advanced Technology, Chinese Academy of Sciences, Shenzhen, China, and South China Agricultural University (E-mail: jiamingmai@163.com).).

Q. Zhu, Y. Xie and L. Wang are with the Shenzhen Institutes of Advanced Technology, Chinese Academy of Sciences, Shenzhen, China (phone: +86-15818569871; Corresponding author: E-mail: qs.zhu@siat.ac.cn).

D. Wu is with the Shenzhen Institutes of Advanced Technology, Chinese Academy of Sciences, Shenzhen, China, and Shanghai Jiao Tong University, Shanghai, China (E-mail: di.wu@siat.ac.cn).).

978-1-4799-7397-2/14/$31.00 © 2014 IEEE

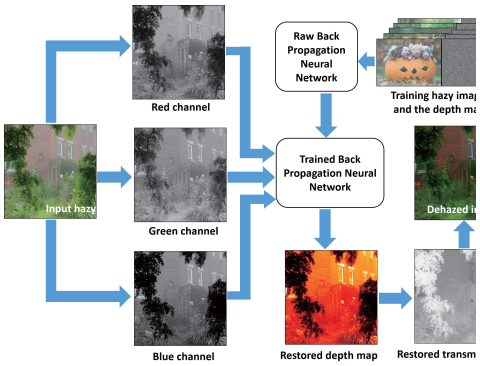

Fig. 2 An overview of the proposed dehazing algorithm.

In this paper, we propose a novel learning-based approach for single image dehazing. The proposed approach is mostly inspired by the observation that the color of the objects fades gradually along with the increment of the scene depth. We regard the RGB values of the pixels within the image as the important feature, and use the back propagation neural network to mine the internal link between color and depth from the training samples, which consists of the hazy images and their corresponding ground truth depth map. With the trained neural network, we can easily restore the depth information as well as the scene radiance from the hazy image. Figure 2 shows an overview of the proposed dehazing algorithm. Experimental results show that the proposed approach can produce a high-quality haze-free image with the single hazy image and achieve the real-time requirement.

The rest of the paper is organized as follows. In Section II, we review the widely used hazy image formation model. In Section III, the color feather that we used for estimating the scene depth is discussed. In Section IV, we introduce the back propagation neural network model for single image dehazing. In Section VI, we illustrate the method of restoring the scene radiance. The experimental results of the proposed dehazing method are shown in Section VI. Finally, we summarize the paper in Section VII.

II. HAZY IMAGE FORMATION MODEL

For describing the formation of the hazy image, the atmospheric scattering model, which was provided by McCartney [23] and further derived by Narasimhan and Nayar [9, 10, 24, 25], has been widely used in previous works. The model can be expressed as below:

$$\mathbf{I}(x) = \mathbf{J}(x)t(x) + \mathbf{A}(1 - t(x)) \tag{1}$$

$$t(x) = e^{-\beta d(x)} \tag{2}$$

where $\mathbf{I}$ is the observed intensity of the hazy image, $\mathbf{J}$ is the scene radiance which describes the haze-free image we want, $\mathbf{A}$ is the global atmospheric light, t is the medium transmission representing the ratio of the portion of the light that reaches the imaging system to the scattered portion, β is the scattering coefficient which can be regarded as a constant in the homogeneous atmosphere, and d is the distance from the scene point to the observer.

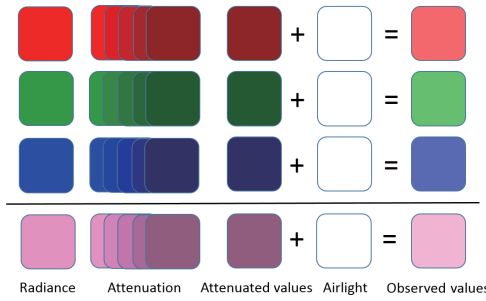

Fig. 3 Changes of intensity during the process of imaging in hazy weather.

The goal of image dehazing is to estimate $\mathbf{J}$ with the single hazy image $\mathbf{I}$:

$$\mathbf{J}(x) = \frac{\mathbf{I}(x) - \mathbf{A}}{t(x)} + \mathbf{A} \tag{3}$$

However, it is actually an ill-posed issue since only I is known while A and t are unknown according to Equation 3. To solve this problem, the input hazy image has to be put to good use.

III. COLOR FEATURE FOR ESTIMATING THE DEPTH

The atmospheric scattering model describes two mechanisms in the process of imaging in hazy weather as reported in [24]. The first mechanism is the direct attenuation of a beam of light as it travels through the atmosphere. The term $\mathbf{J}(x)t(x)$ in Equation 1 is used for describing this mechanism, and it reveal the fact that the intensity of the pixels within the image reduces in a multiplicative manner in the process of attenuation. The second mechanism is the airlight which is caused by the scattering of the environmental illumination and described by the rightmost term $\mathbf{A}(1 - t(x))$ in Equation 1. According to the atmospheric scattering model, the influence of the airlight on the observed values is additive.

Figure 3 shows how the color of the pixel changes in the two mechanisms mentioned above. Due to the influence of the direct attenuation, the RGB values of a certain pixel within the image reduce multiplicatively. This result in the low brightness. On the other hand, as the airlight, whose hue tends to be white or gray, is absorbed by the imaging system, the brightness of the pixel is increased significantly while the saturation of that is reduced sharply. As a result, there will be a great difference between the observed value and the real scene radiance. Fortunately, it is an important clue to estimate the depth of scene as we will illustrate latter.

The degree of the distortion is mostly dependent on the concentration of the scattering medium. Meanwhile, if the concentration is fixed, the scene depth will be the main factor that affects the observed values of the RGB color. Since we can assume that the concentration is fixed in most cases, it will be a strong and inherent relation between the RGB values and the depth of the scene. In order to reveal this relation, we use the back propagation neural network to model the problem.

IV. BACK PROPAGATION NEURAL NETWORK MODEL

The multilayer feed-forward neural network performs non-linear regression from a statistical point of view. Theoretically, it is able to closely approximate any function given enough hidden units and enough training samples. Back propagation neural network, which is widely used in data mining and pattern recognition, can be better used for solving our problem.

In our case, we create a four layers neural network including an input layer, two hidden layers and an output layer. Figure 4 shows the back propagation neural network model we used. In the input layer, there are three neurons which represent the input RGB values of the pixel within the hazy image. Twenty neurons are put into each hidden layer and only one neuron is in the output layer standing for the calculated depth of the corresponding scene point. The sigmoid function is used as the activation function in the hidden layers and the output layer:

$$f(x) = \frac{1}{1 + e^{-x}} \tag{4}$$

A. Training Data Collection

The raw model has to be trained to adapt the problem of image dehazing. Unfortunately, one of the most problem of the proposed method is that the training samples, which consist of hazy images and their corresponding ground truth depth maps, are very difficult to obtain since there is not any reliable mean to measure the depths in outdoor scene. Current depth cameras such as Kinect are not able to acquire the accurate depth information.

In order to get enough training data for learning the neural network model, we use the haze-free images collected from google.com and Flickr.com to produce the depth maps and the hazy images. The process of generating the training samples is illustrated in Figure 5. Firstly, we generate the random depth map d which is with the same size to the given haze-free image. The random depth map is stored as a matrix containing pseudorandom values drawn from the standard uniform distribution on the open interval (0, 1). Secondly, we generate four random numbers k, $\lambda 1$, $\lambda 2$ and $\lambda 3$. The value of k is drawn from the standard uniform distribution on the interval [0.85, 1.0]. $\lambda 1$, $\lambda 2$ and $\lambda 3$ are generated from the normal distribution with mean 0 and standard deviation 5.0. The atmospheric light $\mathbf{A}$ are defined as $[k1, k2, k3]$, where $k1 = k + \lambda 1$, $k2 = k + \lambda 2$ and $k3 = k + \lambda 3$. Finally, we generate the hazy image according to Equation 1 and Equation 2 with the depth map d and the atmospheric light $\mathbf{A}$. It is worth noting that the atmospheric light is not guaranteed to be gray color. For this reason, the values of $k1$, $k2$ and $k3$ may be different. Part of the generated random depth maps and the synthetic hazy images are shown in Figure 5(b) and Figure 5(c).

B. Learning the Neural Network Model

To measure the error of the model, we create the squared loss function as follows:

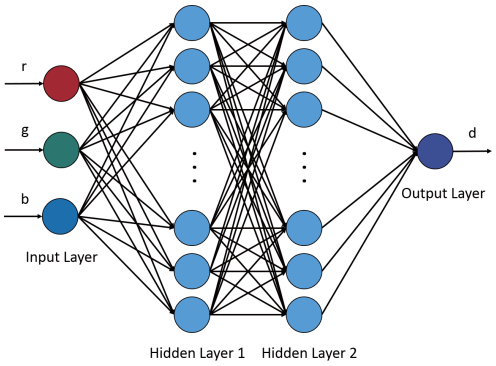

Fig. 4 Back propagation neural network model for image dehazing.

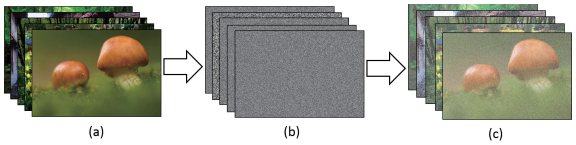

Fig. 5 The process of generating the training samples with the haze-free images. (a) The haze-free images. (b) The generated random depth maps. (c) The generated hazy images.

$$E = \frac{1}{2} \sum_{k \in K} (O_k - d_k)^2 \tag{5}$$

where, K is the total number of the output neurons, O_k is the output of node k in the output layer. To learn the weights of the neuron network, we have to calculate the partial derivative of E with respect to each weight. For the time being, we first concentrate on the weights from the second hidden layer to the output layer and calculate the partial derivative:

$$\begin{aligned} \frac{\partial E}{\partial W_{hk}} &= \frac{\partial}{\partial W_{hk}} \frac{1}{2} \sum_{k_2 \in K} (O_{k_2} - d_{k_2})^2 = (O_k - d_k) \frac{\partial O_k}{\partial W_{hk}} \\ &= (O_k - d_k) f(x_k)(1 - f(x_k)) \frac{\partial x_k}{\partial W_{hk}} \\ &= (O_k - d_k) O_k (1 - O_k) O_h \end{aligned} \tag{6}$$

where W_{hk} is the weight from an arbitrary node h of the second hidden layer to the node k of the output layer, d is the ground truth depth, x_k is the input to the neuron of the output layer, O_h is the output of node h in the second hidden layer, and $f(x)$ is the sigmoid function. For notation purposes, we define δk to be the expression $(O_k - d_k)O_k(1 - O_k)$ and Equation 6 can be rewritten as below:

$$\frac{\partial E}{\partial W_{hk}} = \delta_k O_h \tag{7}$$

Similar to the output layer, we can calculate the partial derivative of E respect to the weights between the first hidden layer and the second one:

$$\begin{aligned} \frac{\partial E}{\partial W_{jh}} &= \frac{\partial}{\partial W_{jh}} \frac{1}{2} \sum_{k \in K} (O_k - d_k)^2 \\ &= O_j O_h (1 - O_h) \sum_{k \in K} \delta_k W_{hk} \end{aligned} \tag{8}$$

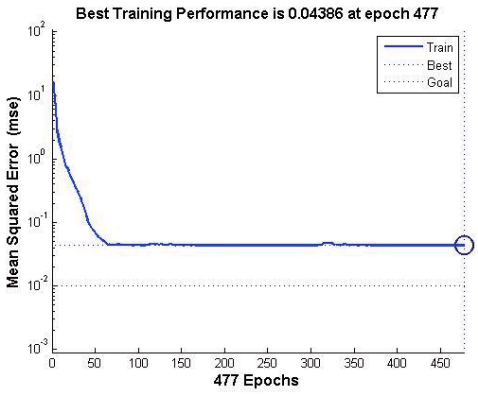

Fig. 6 The training performance of the neural network model.

where W_{jh} is the weight from an arbitrary node j of the first hidden layer to the node h of the second hidden layer, and O_j is the output of node j in the first hidden layer. Setting δh as $O_h(1-O_h)\sum_{k\in K}(\delta_k W_{hk})$, we can rewrite Equation 8 as follows:

$$\frac{\partial E}{\partial W_{jh}} = O_j \delta_h \tag{9}$$

Similarly, we have the following expression:

$$\frac{\partial E}{\partial W_{ij}} = O_i \delta_j \tag{10}$$

where W_{ij} is the weight from the node i of the input layer to the node j of the first hidden layer, δj is defined as $O_j(1-O_j)\sum_{h\in H}(\delta_h W_{jh})$ where H is the total number of the neurons in the second hidden layer. So if we further define l as the certain layer, we can obtain the expression:

$$\frac{\partial E}{\partial W_{l-1,l}} = O_{l-1}\delta_l \tag{11}$$

And it is not difficult to verify that the following expression is also correct:

$$\frac{\partial E}{\theta_l} = \delta_l \tag{12}$$

where θ_l is the basis of the l layer in the neural network. So we are able to use the gradient descent algorithm to learn the weights of the neural network model. The method for updating the weights can be concisely expressed by:

$$\begin{aligned} W_{l-1,l} &= W_{l-1,l} - \eta O_l \delta_l \\ \theta_l &= \theta_l - \eta \delta_l \end{aligned} \tag{13}$$

here η is the rate of learning.

For learning the back propagation neural network model, 60 training samples is used. The training performance of the model is shown in Figure 6. There are 477 epochs in our case and the mean squared error (MSE) is 0.04386.

V. SCENE RADIANCE RESTORATION

After learning the back propagation neural network model, we are able to estimate the depth given a certain pixel within the hazy image. By calculating the depth of each pixel, we can restore the scene depth map of the corresponding hazy image. In other words, the depth d in Equation 2 can be estimated with the help of the neural network model. Assuming that the scattering coefficient β is a constant and equals to 1.0, the transmission t can be calculated as d is known. Thus, the only unknown parameter in the atmospheric scattering model is the atmospheric light **A**.

According to Equation 1 and Equation 2, if the scene depth d tends to be infinity, we have:

$$\begin{aligned} &I(x) = A \\ &s.t.\ d \to +\infty \end{aligned} \tag{14}$$

Equation 14 reveals that the values of the pixel whose scene depth is infinity can stand for the values of the atmospheric light. For this reason, we select the top 0.1% brightest pixels in the scene depth map, and pick out the one that has the highest brightness in the corresponding hazy image as the atmospheric light A. Since A and t are known, we can restore the scene radiance J according to Equation 3 and achieve the goal of dehazing. The method of restoring J is shown as below:

Algorithm 1 An algorithm for enhancing the transmission

Input: the hazy image **I**, the trained network net
Output: dehazed image **J**
Auxiliary functions:
function of splitting the image into three single-channel images: $[r,g,b] = split(I)$
function of estimating the atmospheric light with the RGB channel images: $A = calA(r,g,b,d)$
function of calculating exponent: out = exp(in)
function of estimating depth with net: $d = calD(I, net)$
begin
1: $[r,g,b] = split(\mathbf{I})$;
2: $d = calD(r,g,b,net)$;
3: $beta = 1.0$;
4: $t = exp(-beta * d)$;
5: $\mathbf{A} = calA(\mathbf{I}, d)$;
6: $\mathbf{J} = (\mathbf{I} - \mathbf{A})/t + \mathbf{A}$;
end

VI. EXPERIMENTAL RESULTS

In order to verify the effectiveness of the proposed method, we compare our method with He et al.'s [15, 16], Tarel et al.'s [18] and Nishino et al.'s [20] works. We implemented the four dehazing algorithms in the MatlabR2013a environment on a P4-3.3GH PC with 6GB RAM. For fair comparison, the parameters used in the three algorithms are set to be optimal as [16], [18] and [20]. 180 training images including 60 haze-free images, 60 random depth maps and 60 synthetic hazy images are produced to train the neural network model in our case. The size of each image is 600×400. There are 14.4 million scene points that are used for training.

A. Qualitative Comparison

Figure 7 shows the comparison between the proposed method and Tarel et al.'s method [18]. Figure 7(a) are the input hazy images, Figure 7(b) are the Tarel et al.'s dehazed images, and Figure 7(c) are the results of our method. Figure

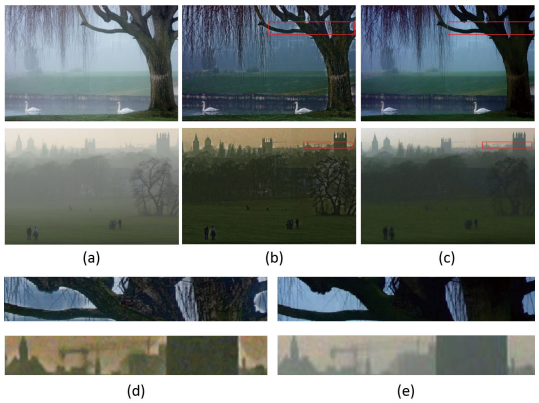

Fig. 7 Comparison with Tarel et al.'s work [18]. (a) The input hazy images. (b) Tarel et al.'s results. (c) Our results. (d) The close-up patches of the images in (b). (e) The close-up patches of the images in (c).

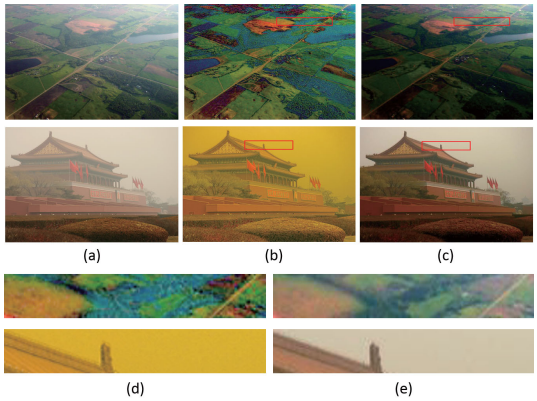

Fig. 8 Comparison with Nishino et al.'s work [20]. (a) The hazy images. (b) Nishino et al.'s results. (c) Our results. (d) The close-up patches of the images in (b). (e) The close-up patches of the images in (c).

7(d) and Figure 7(e) are the close-up patches of the images in (b) and (c) respectively. As we can observe from Figure 7(b) and Figure 7(d), although the dehazing results have recovered most details, it suffers from halos effect since the "median of median filter" used in [18] is not an edge-preserving filter. This can be seen from the branches in the first image and from the distant building in the second image in Figure 7(b) (see also Figure 7(d)). Moreover, due to over enhancement, the results in Figure 7(b) tend to be much darker than it should be. Our results, in contrast, are free from the halos effect as shown in Figure 7(c) and Figure 7(e). The brightness of our dehazed images is more moderate compared with that of Tarel et al.'s.

Figure 8 gives a comparison between our method and Nishino et al.'s method [20]. Figure 8(a) are the hazy images to be dehazing, Figure 8(b) are Nishino et al.'s results, and Figure 8(c) are the results of the proposed method. Figure 8(d) and Figure 8(e) are the close-up patches of the images in (b) and (c) respectively. The dehazed images in Figure 8(b) are with very high contrast and most hazes have been removed. However, the results are over-saturated, especially the second image in Figure 8(b). Obviously, the color of the sky region of the second image in Figure 8(b) are changed

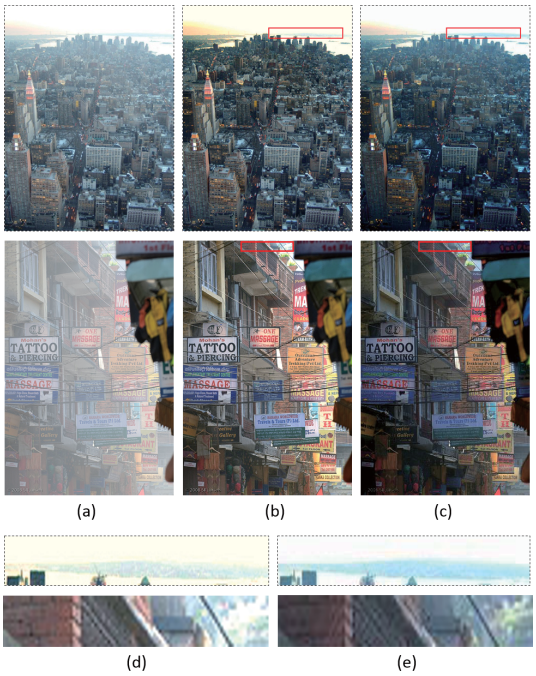

Fig. 9 Comparison with He et al.'s work [15, 16]. (a) The input hazy images. (b) He et al.'s results. (c) Our results. (d) The close-up patches of the images in (b). (e) The close-up patches of the images in (c).

severely (see also Figure 8(d)). This lead to the poor vison effect. Compared with Nishino et al.'s results, our results do not have the problem of over enhancement. The color of the restored scenery objects in our dehazed images is natural and vivid as shown in Figure 8(c) and Figure 8(e).

In Figure 9, we compare our method with He et al.'s method [15, 16]. Figure 9(a) are the input hazy images, Figure 9(b) are the results obtained by He et al.'s method, and Figure 9(c) shows the dehazed images of our method. Figure 9(d) and Figure 9(e) are the close-up patches of the images in (b) and (c) respectively. The dehazing results of He et al.'s method are pleasing as we show in Figure 9(b). There is not any halo effect in the results and hazes in the distance are well removed. Although He et al.'s results are good, the results acquired by the proposed method are even better. It is observed from Figure 9(c) that the detail of the scenery objects that are far away from the observer can be well restored. We are able to see the mountain at the top of the first image and the objects on the right of the flowerpot at the top of the second image in Figure 9(c) (see also Figure 9(e)) while we can hardly see those objects in Figure 9(b) (see also Figure 9(d)). Dark channel prior that is used in He et al.'s approach can be regarded as a powerful feature for detecting hazes in a single image. This feature is actually an important cue that reveals the relation between the color of the scenery objects and its corresponding depth. However, it has a key limitation. That is, it is not suitable for all the regions. The neural network model used in our approach, in contrast, benefits from a large amount of training data and is able to handle most cases. For this reason, the proposed method performs better in terms of the dehazing effect of

the distant regions.

B. Quantitative Comparison

In order to test the efficiency of the proposed method, we run the experiment on the hazy images with different sizes. It takes 1 hour and 11 minutes to train the neural network model with 14.4 million training scene points. Although it needs a long time to finish the off-line training process, the on-line computational complexity of the proposed image dehazing algorithm is reduced greatly with the trained neural network model. The average on-line consuming time is recorded in Table I. Compared with the three methods, our method uses the least time to remove hazes from the images. The proposed dehazing method reduces the computational complexity of the three methods [16, 18, 20] by 97.76%, 99.27% and 99.67% respectively, and achieve the real-time acquirement. This is mainly due to the fact that the proposed method performs in a pixel-wise manner and the operation taken on each pixel is with $O(1)$ complexity. So given an image with the size of $m \times n$, the on-line computational complexity of the proposed algorithm is $O(mn)$.

TABLE I

QUALITY ASSESSMENT DATA TO THE REPRESENTATIVE HAZE REMOVAL METHODS.

Image size	He et al. [15, 16]	Tarel et al. [18]	Nishino et al. [20]	Ours
600×400	10.55s	6.71s	98.34s	0.40s
800×600	18.64s	57.04s	184.77s	0.64s
1024×768	36.89s	69.29s	317.39s	0.75s
1536×1024	73.57s	218.03s	649.72s	1.59s
1803×1080	90.72s	351.13s	861.36s	1.78s
Sum	230.37s	702.20s	2111.68s	5.16s

VII. CONCLUSIONS

In this paper, we have proposed a novel learning-based approach for single image dehazing. We abstract the RGB values of the pixels within the hazy image as the important feature, then use the back propagation neural network to mine the internal link between color and depth from the training samples, which consists of the hazy images and the corresponding ground truth depth map. With the help of the trained neural network model, we are able to easily restore the depth information and the scene radiance from the single hazy image. Experiments show that the proposed approach is able to produce a high-quality haze-free image with the single hazy image and achieve the real-time requirement. For creating a more robust neural network model for single image dehazing, we will focus on finding other useful features such as texture and structure in the future works.

REFERENCES

[1] Qingsong Zhu, Zhan Song, Yaoqin Xie and Lei Wang. "A Novel Recursive Bayesian Learning-Based Method for the Efficient and Accurate Segmentation of Video With Dynamic Background," *IEEE Transactions on Image Processing (TIP)*, vol. 21, no. 9, pp. 3865-3876, 2012.

[2] T. K. Kim, J. K. Paik and B. S. Kang, "Contrast enhancement system using spatially adaptive histogram equalization with temporal filtering," *IEEE Trans. Consumer Electronics* vol. 44, no. 1, pp. 82-87, 1998.

[3] Stark and J. Alex, "Adaptive image contrast enhancement using generalizations of histogram equalization," *IEEE Trans. Image Processing (TIP)*, vol. 9, no. 5, pp. 889-896, 2000.

[4] J. Y. Kim, L. S. Kim and S. H. Hwang. "An advanced contrast enhancement using partially overlapped sub-block histogram equalization." *IEEE Transactions on Circuits Systems for Video Technology (TCSVT)*, vol. 11, no. 4, 2001, pp. 475-484.

[5] Y. Y. Schechner and S. G. Narasimhan, and S. K. Nayar, "Instant dehazing of images using polarization," *in Proc. IEEE Conference on Computer Vision and Pattern Recognition (CVPR)*, 2001.

[6] S. Shwartz, E. Namer, Y. Y. Schechner. "Blind haze separation, " *in Proc. IEEE Conference on Computer Vision and Pattern Recognition (CVPR)*, vol. 2, 2006, pp. 1984-1991.

[7] Y. Schechner, S. Narasimhan and S. Nayar, "Polarization-based vision through haze," *Applied Optics*, vol. 42 no. 3, pp. 511 -525, 2003.

[8] S. G. Narasimhan and S. K. Nayar. "Chromatic framework for vision in bad weather," *in Proc. IEEE Conference on Computer Vision and Pattern Recognition (CVPR)*, 2000.

[9] S. K. Nayar and S. G. Narasimhan. "Vision in bad weather," *in Proc. IEEE International Conference on Computer Vision (ICCV)*. vol. 2, 1999.

[10] S. G. Narasimhan and S. K. Nayar. "Contrast restoration of weather degraded images," *IEEE Trans. Pattern Analysis and Machine Intelligence (TPAMI)*, vol. 25, no.6, pp. 713-724, 2003.

[11] S. G. Narasimhan and S. K. Nayar, "Interactive (de) weathering of an image using physical models," *IEEE Workshop on Color and Photometric Methods in Computer Vision*. vol. 6, no. 4, France, 2003.

[12] J. Kopt, B. Neubert, B. Chen, M. Cohen and D. Cohen-Or. "Deep photo: Model-based photograph enhancement and viewing," *ACM Transactions on Graphics (TOG)*, vol. 27, no. 5, pp. 116, 2008.

[13] R. T. Tan, "Visibility in bad weather from a single image," *in Proc. IEEE Conference on Computer Vision and Pattern Recognition (CVPR)*, 2008, pp. 1-8.

[14] R. Fattal, "Single image dehazing," *ACM Transactions on Graphics (TOG)*, vol. 27, no. 3, pp. 72, 2008.

[15] K. He, J. Sun, and X. Tang, "Single image haze removal using dark channel prior," *IEEE Trans. Pattern Analysis and Machine Intelligence (TPAMI)*, vol. 33, no. 12, pp. 2341-2353, 2011.

[16] K. He, J. Sun and X. Tang, "Guided image filtering," *IEEE Trans. Pattern Analysis and Machine Intelligence (TPAMI)*, vol. 35, no. 6, pp. 1397-1409, 2013.

[17] J. P. Tarel, and H. Nicolas, "Fast visibility restoration from a single color or gray level image," *in Proc. IEEE Conference on Computer Vision (ICCV)*, 2009, pp. 2201-2208.

[18] J. P. Tarel, N. Hautire, L. Caraffa, A. Cord, H. Halmaoui and D. Gruyer, "Vision enhancement in homogeneous and heterogeneous fog," *IEEE Trans Intelligent Transportation Systems Magazine*, vol. 4, no. 2, pp. 6-20, 2012.

[19] L. Kratz, and K. Nishino, "Factorizing scene albedo and depth from a single foggy image," *in Proc. IEEE Conference on Computer Vision (ICCV)*, 2009, pp. 1701-1708.

[20] K. Nishino, L. Kratz, and S. Lombardi, "Bayesian defogging," *International Journal of Computer Vision (IJCV)*, vol. 98, no. 3, pp. 263-278, 2012.

[21] Q. Zhu, L. Shao, Q. Li, Y. Xie. "Recursive Kernel Density Estimation for Modeling the Background and Segmenting Moving Objects," In Proceedings of the IEEE ICASSP, pp. 1769-1772. Vancouver. 2013.

[22] Q. Zhu, Z. Zhang, Z. Song, Y. Xie, L. Wang, A Novel Nonlinear Regression Approach for Efficient and Accurate Image Matting, IEEE Signal Processing Letters, vol. 20, no. 11, pp. 1078-1081, 2013.

[23] E. J. McCartney, "Optics of the atmosphere: scattering by molecules and particles," New York, John Wiley and Sons, Inc. 1976.

[24] S. G. Narasimhan and S. K. Nayar. "Vision and the atmosphere," *International Journal of Computer Vision (IJCV)*, vol. 48, no. 3, pp. 233-254, 2002.

[25] S. G. Narasimhan and S. K. Nayar, "Removing weather effects from monochrome images," *in Proc. IEEE Conference on Computer Vision and Pattern Recognition (CVPR)*, 2001